PNAS RESEARCH ARTICLE | AGRICULTURAL SCIENCES

Divergent amplifications of CYP9A cytochrome P450 genes provide two noctuid pests with differential protection against xenobiotics

Yu Shi[a,1], Qingqing Liu[a,1], Wenjie Lu[a], Jing Yuan[a], Yihua Yang[a], John Oakeshott[b], and Yidong Wu[a,2]

Edited by Fred Gould, North Carolina State University, Raleigh, NC; received May 24, 2023; accepted August 7, 2023

Here, we provide mechanistic support for the involvement of the CYP9A subfamily of cytochrome P450 monooxygenases in the detoxification of host plant defense compounds and chemical insecticides in *Spodoptera exigua* and *Spodoptera frugiperda*. Our comparative genomics shows that a large cluster of *CYP9A* genes occurs in the two species but with significant differences in its contents, including several species-specific duplicates and substantial sequence divergence, both between orthologs and between duplicates. Bioassays of CRISPR-Cas9 knockouts of the clusters show that, collectively, the CYP9As can detoxify two furanocoumarin plant defense compounds (imperatorin and xanthotoxin) and insecticides representing three different chemotypes (pyrethroids, avermectins, and oxadiazines). However, in vitro metabolic assays of heterologously expressed products of individual genes show several differences between the species in the particular CYP9As with activities against these compounds. We also find that the clusters show tight genetic linkage with high levels of pyrethroid resistance in field strains of the two species. We propose that their divergent amplifications of the CYP9A subfamily have not only contributed to the development of the broad host ranges of these species over long evolutionary timeframes but also supplied them with diverse genetic options for evolving resistance to chemical insecticides in the very recent past.

spodopteran pests | host adaptation | insecticide resistance | cytochrome P450 | xenobiotic detoxification

Herbivorous insects are exposed to a wide variety of allelochemicals, including some highly toxic defense compounds produced by their host plants, and evidence is accumulating that their capacity to detoxify these chemicals is key to their ability to utilize both the types of host tissue and the range of host species they will use (1–4). Their detoxification capacity depends in large part on gene/enzyme systems in superfamilies such as the P450 monooxygenases (P450s), uridine diphosphate-glycosyltransferases, carboxyl/cholinesterases, and glutathione-S-transferases, which help them sequester or metabolize the toxicants (5–8). The amplification and diversification of genes in particular subfamilies of these superfamilies encoding enzymes with intrinsically promiscuous substrate ranges have been associated, both with the accumulation of new hosts over long evolutionary timeframes (4, 9–13) and with tolerance of, and/or development of resistance to, synthetic pesticides over the last 70 y (14–18).

The research to date has most often implicated P450s in these processes (17). For example, the diversification of the CYP9Q subfamily has been implicated in the tolerance of many bee species to neonicotinoid and butenolide insecticides (15, 19), while amplification of a member of the CYP6CY subfamily has been implicated in the expansion of the aphid *Myzus persicae* into tobacco and, by enhancing its tolerance, also preadapted it to resist neonicotinoid insecticides (10). Several other P450s from various subfamilies have also now been identified as candidate resistance genes against various insecticides on the basis of their biochemical competencies and expression profiles on exposure to the compounds (17, 20–22), with some of them also proposed to act against plant defense chemicals which can be detoxified in overlapping metabolic pathways (10, 23, 24) and induce similar changes in gene expression (25). These overlaps have led to a "preadaptation hypothesis" (26, 27) which links the long-term macroevolution of insects' host ranges and their short-term microevolution of insecticide tolerance. However, direct mechanistic evidence linking these evolutionary outcomes to changes in the properties of particular members of the four enzyme superfamilies remains scant, even for the P450s.

The noctuid moth genus *Spodoptera* is a promising model for testing these mechanistic links. About half of the 31 spodopteran species known (28) are important agricultural pests, and many of them are highly polyphagous species which can feed on more than 100 host plants species, commonly including major crops such as maize, rice, and cotton

Significance

We provide mechanistic evidence linking a cluster of rapidly diverging cytochrome P450 genes in two insect pests to their ability to utilize diverse host plants and their propensity to evolve insecticide resistance. CRISPR-Cas9 technology, bioassays, and biochemical assays show that amplified CYP9As in *Spodoptera exigua* and *Spodoptera frugiperda* collectively metabolize furanocoumarin plant defense compounds and pyrethroid, avermectin, and oxadiazine insecticides but with many differences between the species in the particular CYP9As with activity against these compounds. Further, pyrethroid resistance in both species cosegregates with the amplified gene cluster in genetic crosses. We suggest that the cluster has contributed to both the long-term macroevolution of these polyphagous insects to diverse hosts and preadapted them for short-term microevolution of insecticide resistance.

Author contributions: Y.S., Y.Y., and Y.W. designed research; Y.S., Q.L., W.L., and J.Y. performed research; Y.S., Q.L., Y.Y., J.O., and Y.W. analyzed data; and Y.S., J.O., and Y.W. wrote the paper.

The authors declare no competing interest.

This article is a PNAS Direct Submission.

[1]Y.S. and Q.L. contributed equally to this work.

[2]To whom correspondence may be addressed. Email: wyd@njau.edu.cn.

This article contains supporting information online at https://www.pnas.org/lookup/suppl/doi:10.1073/pnas.2308685120/-/DCSupplemental.

Published September 5, 2023.

(https://www.cabi.org/cpc/). High levels of resistance have also been reported to almost all chemical insecticide families in the four most studied species, namely the fall armyworm *Spodoptera frugiperda*, the beet armyworm *Spodoptera exigua* (Hübner), the African cotton leafworm *Spodoptera littoralis* (Bosiduval), and the tobacco cutworm *Spodoptera litura* (Fabricius) (http://www.pesticideresistance.org). Although documented cases of target site resistance are increasing as well (29–31), the evidence overall suggests that metabolism by detoxification enzymes is the major resistance mechanism in these pests (20). Furthermore, the evidence overall shows that cytochrome P450s are most commonly implicated (12, 32) and several subfamilies within the CYP3 and CYP4 clans of P450s are the most expanded of the major detoxification systems across the four species (33).

In particular, the CYP9A subfamily stands out as having undergone several recent duplications, both in these four species (33) and in a related noctuid pest, the cotton bollworm *Helicoverpa armigera* (34). Many of these genes are induced by xenobiotics (33, 34), and some are constitutively overexpressed in resistant strains (35, 36). A small region of the genome including a CYP9A gene cluster has also been found to be positively selected in a deltamethrin-resistant strain of *S. frugiperda* (37). These findings suggest that this P450 subfamily might play a key role in both the detoxification of exogenous compounds and evolution of insecticide resistance but do not yet establish a functional basis for the associations.

Here, we focus on the CYP9A subfamily in *S. frugiperda* and *S. exigua*, which are only relatively distantly related within the genus *Spodoptera* (28). We first characterized the complements of the subfamily in each species by careful manual annotation of the genomes and PCR validations where required. Fourteen genes were found in *S. frugiperda* and eleven in *S. exigua*, with all but one in each species located in a single cluster. CRISPR-Cas9 knockout technology and bioassays were then used to evaluate the contributions of the cluster in each species to their detoxification of diverse phytochemicals and insecticides. These results confirmed large contributions of the clusters to the detoxification of certain compounds, so we then used tissue-specific transcriptomics and in vitro biochemical assays of heterologously expressed products of the component genes to identify the specific genes involved. This showed several differences between the species in the particular genes whose products had relevant activities. Finally, genetic linkage analysis was used to establish the role of the clusters in pyrethroid resistance in field populations of the two species. Our findings demonstrate a mechanistic link between some members of the CYP9A subfamily and both host plant adaptation and resistance evolution in the two species but also point to several differences between the species in the specific genes likely to be involved.

Results

Genomic Organization and Phylogeny of the CYP9A Subfamily. The complements of CYP9A genes in wild-type strains of the two species were compiled from two chromosome-level genomes for each of *S. frugiperda* (GenBank Nos GCF_011064685.1 and GCA_019297735.1) and *S. exigua* (GenBank Nos GCA_011316535.1 and GCA_902829305.4).

The subfamily was found to comprise 14 genes in *S. frugiperda* and 11 in *S. exigua*. This compares with the 13 reported in *S. litura* (38), which is more closely related to *S. frugiperda* than *S. exigua* (Fig. 1). All but one of the genes in all three species was located in a large cluster (~84, ~108, and ~114 kb in *S. frugiperda, S. exigua,* and *S. litura*, respectively), with the other one on a different chromosome in each case. All but one terminal gene in each species' cluster was arranged in head (HD)-to-tail orientation, and the similarities of flanking genes confirmed the syntenic arrangements of both the cluster and the remote singleton gene in the three species.

One of the HD-to-tail genes in *S. frugiperda*, *SfCYP9A77*, had not been reported previously. We found that it lay between *CYP9A32* and *CYP9A31* in one reference genome (GenBank No.

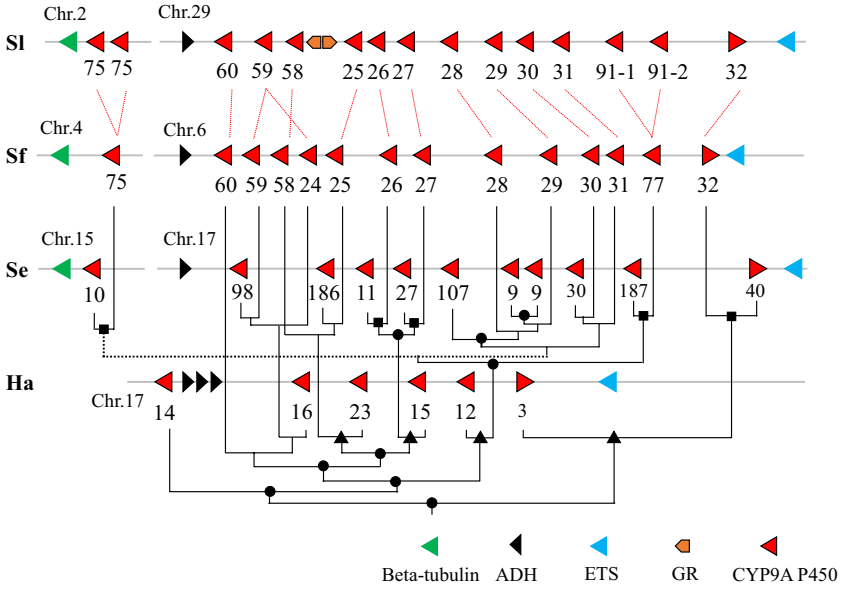

Fig. 1. Complements and phylogeny of the CYP9A subfamily of P450 genes in *S. litura* (Sl), *S. frugiperda* (Sf), *S. exigua* (Se), and *H. armigera* (Ha). The CYP9A genes in the four species are shown in their correct orientation and order but physical distances are not to scale. The phylogenetic tree (produced in full in *SI Appendix*, Fig. S2) is superimposed with its correct topology, but with branch lengths modified here for clarity. Gene duplications not associated with species splits are indicated with ●, and those linked to the *H. armigera*/*Spodoptera* and *S. exigua*/*S. frugiperda* splits are indicated with ▲ and ■, respectively. Other presence/absence differences for which the order of events was less clear or most easily explained by gene losses (e.g., the absence of a clear orthologue of *SfCYP9A31* and *SlCYP9A31* in *S. exigua*; see also *SI Appendix*, Fig. S2) are left unmarked. For simplicity, pairs of orthologous genes in the closely related *S. frugiperda* and *S. litura* are just linked by red dotted lines. The annotated flanking genes encoding Beta-tubulin, alcohol dehydrogenases (ADH), E26 transformation-specific (ETS) transcription factor, and gustatory receptor (GR) are also shown.

GCF_011064685.1) (39) but was missing in the other (GenBank No. GCA_019297735.1) (37) (*SI Appendix*, Fig. S1*A*). Its position in the genome of the YJ-19 *S. frugiperda* strain was confirmed by PCR and Sanger sequencing (*SI Appendix*, Fig. S1 *B* and *C*). We also found a previously unreported HD-to-tail gene in the *S. exigua* cluster, an adjacent, identical copy of *SeCYP9A9*, in both its reference genomes. Quantitative PCR showed a 2.35 ± 0.04 fold higher copy number for *SeCYP9A9* than for the adjacent *SeCYP9A107* gene and the existence and position of the duplication was confirmed by Sanger sequencing.

Few cases of 1:1:1 orthologies occurred across all three species' CYP9A genes but five 1:1 cases, including the remote singleton gene (*SfCYP9A75* and *SeCYP9A10* in *S. frugiperda* and *S. exigua*, respectively) and the terminal, opposite orientation gene in the cluster (*SfCYP9A32* and *SeCYP9A40*, respectively), were identified when just *S. frugiperda* and *S. exigua* were considered. Inferred amino acid sequence identities between the *S. frugiperda* and *S. exigua* orthologs varied from 49.7% for *SeCYP9A40* and *SfCYP9A24* up to 92.3% for *SfCYP9A75* and *SeCYP9A10*. Inferred amino acid sequence identities (Dataset S1) among CYP9A paralogs were 50 to 89% and 52 to 81% (excepting the duplicated *SeCYP9A9*) in *S. frugiperda* and *S. exigua*, respectively.

The first split in the phylogeny of the subfamily (Fig. 1 and *SI Appendix*, Fig. S2) involved the terminal, opposite orientation genes *SfCYP9A32* and *SeCYP9A40*, which was followed by one generating the genes now located at or near the other end of the cluster (*SfCYP9A60*, *SfCYP9A59* and *SfCYP9A24*, and *SeCYP9A98*). The duplication to the other chromosome (*SfCYP9A75* and *SeCYP9A10*) occurred at a later step in the proliferation of the cluster. While some duplication events involving orthologous pairs of genes in the two species predated the separation of the species, there were also several other genes in *S. frugiperda* and one, the *SeCYP9A9* duplication, in *S. exigua*, which lacked obvious orthologs; these represent gene gain or loss events that occurred after the species separated. While some of the differences, most obviously the *SeCYP9A9* duplication, are best interpreted as gene gains, the full phylogeny (*SI Appendix*, Fig. S2) suggests others, such as the missing ortholog of *SfCYP9A31* in *S. exigua*, are most easily explained as gene loss events.

Knockouts of the Cluster Confirm Its Role in Chemical Defense. The dual sgRNA (single guide RNA)-directed CRISPR-Cas9 system was employed to delete all of the CYP9A gene cluster from the WH-S *S. exigua* and YJ-19 *S. frugiperda* strains, from which the respective homozygous knockout strains WH-d9A (Fig. 2 *A*–*C*) and YJ-d9A (Fig. 3 *A*–*C*), respectively, were created (*SI Appendix*, Table S1). Responses of larvae from the knockout and parent strains to two phytochemicals and eight insecticides covering a wide range of chemical structures were then determined (Figs. 2*D* and 3*D* and *SI Appendix*, Tables S2 and S3). Compared to the corresponding parent strains, both knockout strains were significantly more susceptible to two of the insecticides, esfenvalerate (22 and 42 fold lower LC_{50} values for WH-d9A and YJ-d9A, respectively) and abamectin (5 and 15 fold, respectively), and WH-d9A was also more susceptible to the phytochemical imperatorin (5 fold) and YJ-d9A to the insecticide indoxacarb (12 fold) and, to a lesser extent, the other phytochemical, xanthotoxin (2.5 fold). No significant differences from the corresponding parent strains were found for emamectin benzoate, chlorantraniliprole, spinosad, chlorfenapyr, or chlorpyrifos.

Functional Assays of Individual CYP9A Enzymes. qRT-PCR assays were used to compare constitutive expression levels of the various CYP9A genes in four larval organs that have been implicated in defense functions, namely the midgut (MG), fat body (FB), Malpighian tubules (MTs), and HD (7). We found large differences (>2,000 fold in some cases) in those levels across the four organs in the susceptible strain of each species (Fig. 4). Genes showing relatively high expression in all four organs included the orthologs *SeCYP9A40* and *SfCYP9A32*, which arose from the oldest split in the phylogeny, plus *SfCYP9A31* (in particular) and *SeCYP9A10*, which were not orthologs but only split much later in the phylogeny. On the other hand, *SeCYP9A187*, in another clade, was also relatively highly expressed in the four tissues but expression of its ortholog, *SfCYP9A77*, was relatively low in all four organs. Of the genes with more organ-specific expression profiles, two other orthologous pairs, *SfCYP9A27* and *SeCYP9A27* and *SfCYP9A26* and *SeCYP9A11*, all in the same clade, all showed higher expression in the MG than the other tissues, whereas the higher expression of *SeCYP9A186* in MTs was not matched by either of its closest relatives in *S. frugiperda*, *SfCYP9A25* and *SfCYP9A58*.

A baculovirus-mediated expression system in Sf9 cells was then used to express all 24 distinct CYP9A genes of *S. frugiperda* and *S. exigua* in vitro. The quality and content of the recombinant P450s produced were indicated by their reduced CO-difference spectra (*SI Appendix*, Fig. S3). Their activities were then tested for compounds for which the knockout results above suggested the cluster had most activity (Fig. 4).

Seven of the ten *S. exigua* P450s, covering a wide range of the CYP9A clades, metabolized imperatorin, with SeCYP9A11 showing the highest activity, 0.85 ± 0.02 pmol/min/pmol P450. Only three of the fourteen *S. frugiperda* P450s metabolized xanthotoxin, but they all did so at rates approaching that of the most active of the *S. exigua* P450s against imperatorin, with the highest being 0.62 ± 0.03 pmol/min/pmol P450 for SfCYP9A24.The three xanthotoxin-active *S. frugiperda* P450s lay in two well-separated clades, both of which also contained imperatorin-active *S. exigua* P450s.

Esfenvalerate was metabolized by eight *S. exigua* and eleven *S. frugiperda* CYP9As. The enzymes with the highest activity in each species, SeCYP9A40 and SfCYP9A32, were orthologs from the oldest clade but the two next highest in the two species (SeCYP9A11, SeCYP9A27, SfCYP9A28, and SfCYP9A29) were not orthologs and lay in much younger clades. Summed across the 4′- and 2′-hydroxy-metabolites, the activities of SeCYP9A40 and SfCYP9A32 were 0.66 and 0.24 pmol/min/pmol P450, respectively. The 4′-hydroxy-esfenvalerate metabolite was the major product detected in the assays of all the esfenvalerate-active enzymes except SfCYP9A75 and SeCYP9A107. Interestingly, however, those cases where 2′-hydroxy-esfenvalerate was also produced in significant amounts, namely the SeCYP9A9 duplicates, SeCYP9A107, SfCYP9A28 and SfCYP9A29, were all closely related to one another in the same recently evolved clade.

Only one *S. exigua* enzyme, SeCYP9A40, again the one from the oldest clade, metabolized abamectin, at a rate of 5.22 ± 0.02 pmol/min/pmol P450. Three *S. frugiperda* P450s metabolized abamectin, one being SfCYP9A32, i.e., the ortholog of the active *S. exigua* enzyme, and the others, SfCYP9A26 and SfCYP9A27, both lying in the same, younger clade. Activities of the three *S. frugiperda* P450s ranged from 0.82 to 2.4 pmol/min/pmol P450.

Indoxacarb was metabolized by seven *S. frugiperda* CYP9As which were widely scattered across the phylogeny. SfCYP9A31 yielded the highest activity, 0.45 pmol/min/pmol P450, but SfCYP9A29, SfCYP9A77, and SfCYP9A32 activities were also quite high.

Collating the expression and activity data reveals that the old orthologs SeCYP9A40 and SfCYP9A32 both have relatively high expression in all four organs, the highest activity in their respective species for esfenvalerate, and the highest P450 or second highest activities for abamectin. Similarly, the other highly and widely

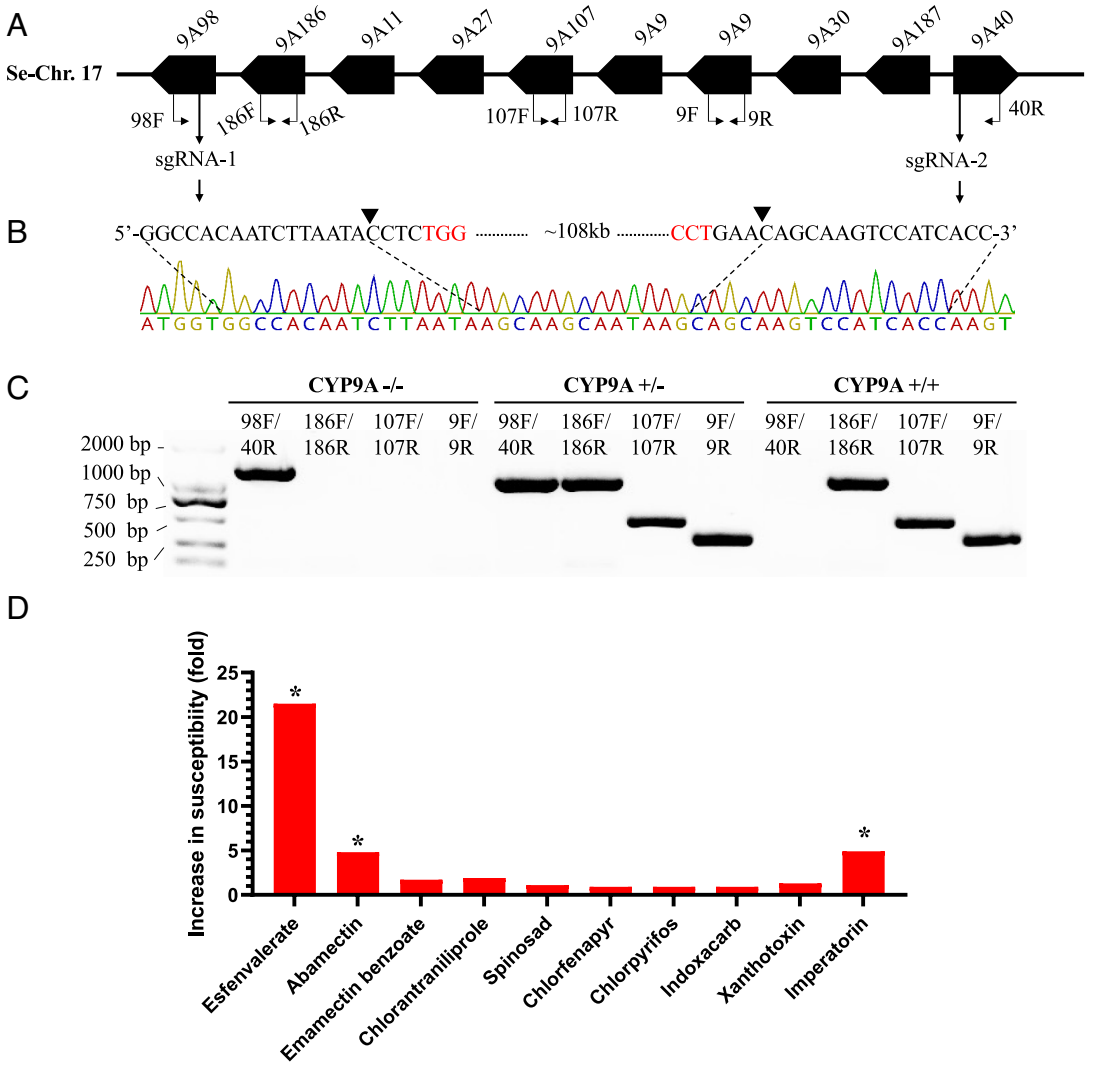

Fig. 2. CRISPR-Cas9 mediated knockout of the CYP9A cluster of *S. exigua* and responses of the knockout strain WH-d9A to phytochemical toxins and insecticides. (*A*–) Positions of the two sgRNAs and the primer pairs for allele-specific PCR detection. The ten CYP9As are shown in their correct orientation and order, but their lengths and distances apart are not shown to scale. (*B*) Target sequences of the two sgRNA, the PAM sequences (red), and a representative chromatogram of direct sequencing of PCR products of individuals from the WH-d9A strain with the primer pairs 98F/40R. The cleavage sites are indicated with black triangles. (*C*) shows how individual *S. exigua* carrying deletions of the CYP9A cluster could be detected from the banding patterns of PCR products amplified with diagnostic primer pairs. (*D*) shows the fold increases in susceptibility of the knockout vs. wild type strains. The asterisks indicate significant differences (i.e., nonoverlapping 95% fiducial limits) in LC_{50}s.

expressed *S. frugiperpa* enzyme, SfCYP9A31, has the highest activity against indoxacarb. However, the other two highly and widely expressed *S. exigua* enzymes, SeCYP9A187 and SeCYP9A10, have low or no activity against all the measured toxins. Two of the enzymes showing more organ-specific high expression, SeCYP9A11 and SfCYP9A27, which are heavily expressed in the MG, have relatively high activities against imperatorin and abamectin, respectively, but SeCYP9A186, which is highly expressed in MTs, has only modest or negligible activities against the toxins tested. Notably also, the *S. frugiperda* enzyme with the highest xanthotoxin activity, SfCYP9A24, is not highly expressed in any of the four organs.

Associations with Insecticide Resistance in Field Populations. Bioassays of parental strains and F_1 progeny of reciprocal crosses between resistant and susceptible strains of each species were then carried out to determine the mode of inheritance of esfenvalerate resistance (Table 1). The susceptible strain used in these crosses was the original wild-type strain WH-S for *S. exigua,* but for *S. frugiperda*, we used the knockout strain YJ-d9A. Survival rates of the F_1s from each cross exposed to the fenvalerate closely approached those seen in the resistant parental strain, indicating that the trait was essentially fully dominant in both species. Given that larvae of both sexes would have been included in the bioassays, and that mortality did not differ significantly between the reciprocal crosses (P = 0.12 for *S. exigua* and P = 0.99 for *S. frugiperda*, Fisher's exact test), there was also no evidence for either sex linkage or maternal effects.

To test for genetic linkage between resistance and the cluster we then analyzed the progeny of backcrosses between the F_1s that had survived the esfenvalerate treatment and the respective susceptible parental strains. Two cohorts of backcross individuals from each cross were genotyped for the CYP9A cluster by PCR. For each species, a control cohort comprised untreated larvae and this showed the expected 1:1 ratio of heterozygotes for the two cluster haplotypes and homozygotes for the susceptible cluster haplotype, whereas the test cohort comprised larvae that had survived a treatment with esfenvalerate and this cohort only contained heterozygotes (Table 2, $P < 0.01$ for each species, Fisher's exact test). Although the sample sizes for the test cohorts were

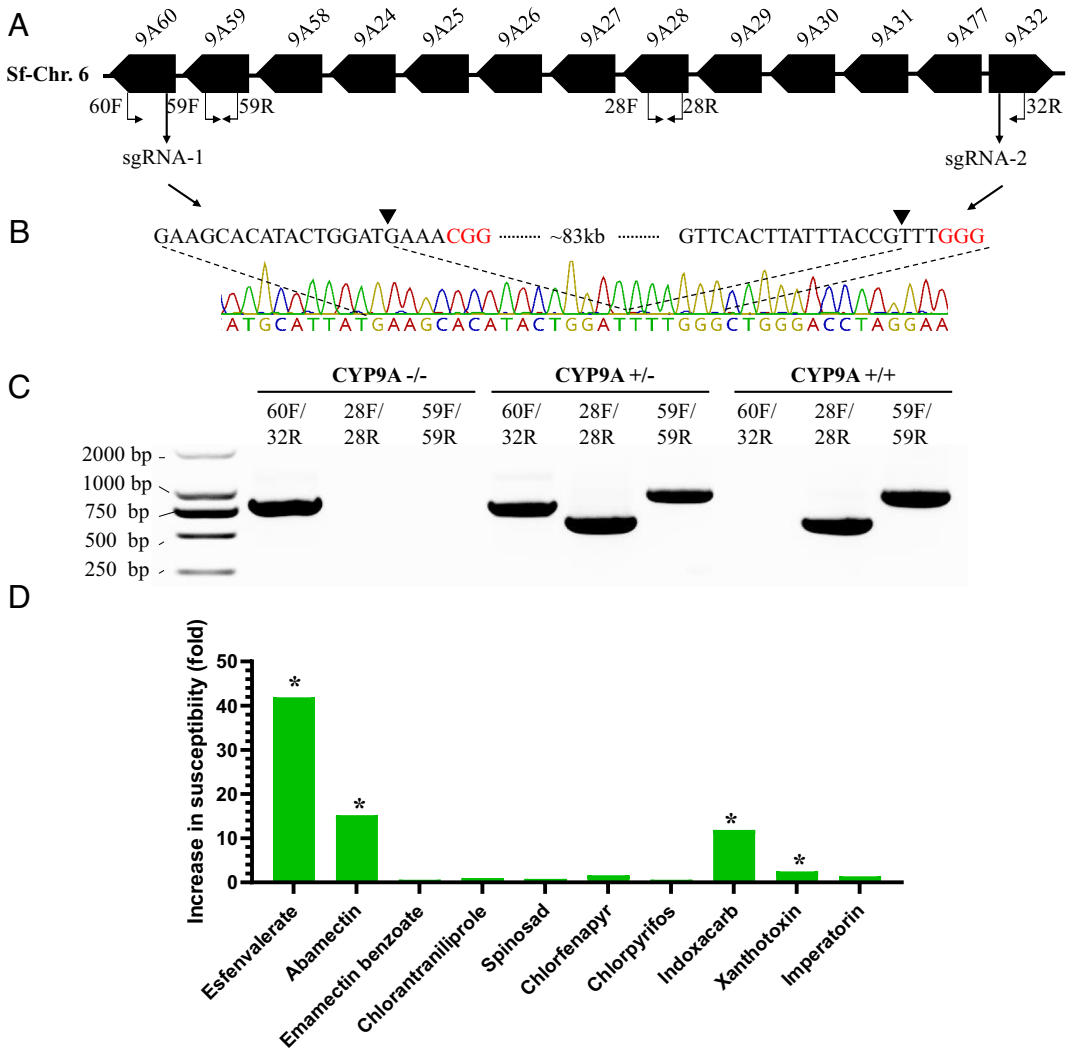

Fig. 3. CRISPR-Cas9 mediated knockout of the CYP9A cluster of *S. frugiperda* and responses of the knockout strain YJ-d9A to phytochemical toxins and insecticides. (*A*) Positions of the two sgRNAs and the primer pairs for allele-specific PCR detection. The 13 CYP9As are shown in their correct orientation and order, but their lengths and distances apart are not shown to scale. (*B*) Target sequences of the two sgRNA, the PAM sequences (red), and a representative chromatogram of direct sequencing of PCR products of individuals from the YJ-d9A strain with the primer pairs 60F/32R, respectively. The cleavage sites are indicated with black triangles. (*C*) shows how individual *S. frugiperda* carrying deletions of the CYP9A cluster could be detected from the banding patterns of PCR products amplified with diagnostic primer pairs. (*D*) shows the fold increases in susceptibility of the knockout vs. wild type strains. The asterisks indicate significant differences (i.e., nonoverlapping 95% fiducial limits) in LC_{50}s.

small—only 40 individuals in total—they thus show a complete association across the two species and their various genetic backgrounds between surviving the esfenvalerate treatment and the presence of the *CYP9A186* haplotype inherited from the resistant parental strain.

Discussion

Our comparisons of CYP9A gene complements revealed that several gain or loss events have occurred in one or other of *S. exigua* and *S. frugiperda* since they diverged about 16 Mya, with several also since *S. frugiperda* diverged from the more closely related *S. litoralis* in the ~12 My since those two species diverged (28). We also found 8 to 13% amino acid sequence divergence between 1:1 orthologs in *S. frugiperda* and *S. exigua*. Given that single amino acid changes in key active site residues can effect qualitative changes in the activities of P450s against particular substrates (36, 40–44), this suggests considerable scope for functional divergence between orthologs of the two species. Similarly, the 11 to 38% sequence divergence within four *S. frugiperda*–specific duplications indicates considerable scope for functional divergence among paralogs. On the other hand, one *S. exigua*–specific duplication involves two copies of *SeCYP9A9* which are identical even in their synonymous sites, indicating duplication events have continued into the very recent past, possibly even as a result of sustained pesticide pressure over the last few decades.

In broad terms, our data support earlier analyses of noctuid and other insect genomes showing "blooms" in gene numbers in certain "unstable" P450 subfamilies (45–49). Consistent with those analyses, however, our phylogeny suggests that while some species-specific CYP9A duplicates represent gene gain events, there are also a few that reflect the loss of an ortholog in the other species compared.

The complements of the CYP9A subfamily in all three of the spodopterans compared here are larger than those of most other lepidopterans studied to date (34). Given that all three species are highly polyphagous, our data thus bear out a more general positive relationship proposed between detoxification gene numbers and host range among *Lepidoptera* (4). This relationship now generally holds true across over twenty species sequenced to date, albeit with

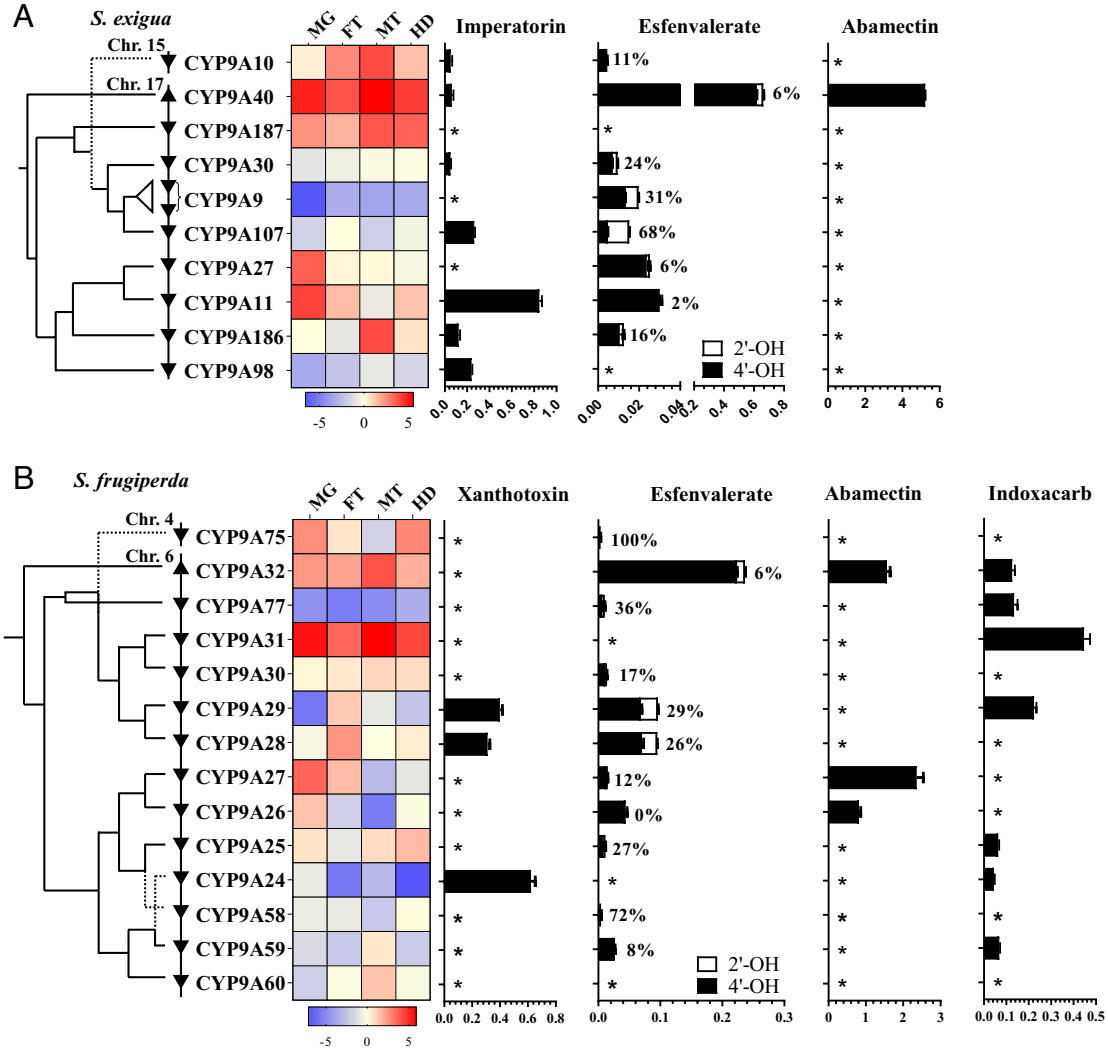

Fig. 4. Phylogenetic relationships, physical organization in genome sequences, relative expression levels in four detoxification organs, and metabolic activity against certain plant toxins and insecticides of CYP9A P450s in *S. exigua* (*A*) and *S. frugiperda* (*B*). The dotted lines in the phylogenies show the major rearrangements. The heat maps were generated using log2-transformed expression ratios relative to the median of all the CYP9A P450s in each species. Red means high expression levels. MG = midgut, FT = fat body, MT = Malpighian tubules, HD = head. Metabolic activity is expressed as pmol/min/pmol P450. For esfenvalerate, activity is based on the summed amounts of the 4′ and 2′ metabolites (black and clear, respectively), with the percentage of the latter also shown. * indicates no detectable activity. Error bars represent mean values ± SEM (n = 3 to 9).

a few exceptions (see also ref. 34); two other major polyphagous lepidopteran pests, *H. armigera* and *Heliothis virescens*, only have moderate numbers of CYP9A genes and the only other species in the order with *CYP9A* complements comparable to the three spodopterans' are another polyphagous moth, *Arctia plantaginis*, and a relatively specialized butterfly *Calyopis cecrops* (34). However, the latter itself may be instructive since the species uses dead leaves from sumac and related trees which contain high levels of tannins and allergens (50). Thus, it may also be exposed to relatively high levels of toxic secondary compounds.

In light of the results for the spodopterans and heliothines above, it would be interesting now to determine the size of the CYP9A subfamily in congeneric species with substantially narrower host ranges, such as *Spodoptera exempta*, *Helicoverpa assulta,* or *Helicoverpa gelotopoeon* (51, 52). Notably also, although they are also pests which are subject to some chemical insecticide controls, none of the latter species have developed major insecticide resistance issues either (51).

A versatile detoxification role for the subfamily in *S. frugiperda* and *S. exigua* was confirmed by the increased sensitivities of our knockout strains for the CYP9A cluster to the two plant defense compounds and three of the eight insecticides tested. The defense compounds are both furanocoumarins but the three insecticides, the pyrethroid esfenvalerate, the oxadiazine indoxacarb, and the macrolide abamectin, are from different chemotypes. The tolerance ratios were not high for the two defense compounds, the highest being 2.5 for the former against xanthotoxin and 4.9 for the latter against imperatorin, but were higher, ~12 to 42 fold, for the three insecticides.

Moreover, our biochemical analyses suggest that more CYP9As could contribute to the detoxification in the two spodopterans than might be expected from work on other species. For example, while just two CYP6AE P450s of *H. armigera* have previously been implicated in indoxacarb metabolism (24), we find that nine of the *S. frugiperda* CYP9As can metabolize this compound. Likewise, only one P450, CYP392A16, has so far been found to be associated with abamectin metabolism and resistance in the spider mite *Tetranychus urticae* (53), but we find that four CYP9As across the two spodopteran species can metabolize abamectin.

Table 1. Inheritance of esfenvalerate resistance in resistant strain of *S. exigua* and *S. frugiperda*

Insects	Strain/Cross	N*	Survival (%)	Dominance Value (*h*)
S. exigua	WH-S	48	0	
	FX-19	72	100	
	FX-19(♂) × WH-S(♀) (F_{1a})	93	97.8	0.98
	FX-19(♀) × WH-S(♂) (F_{1b})	117	92.3	0.92
	F_1 pooled	210	94.8	0.95
S. frugiperda	YJ-d9A	48	0	
	AQ-22	48	100	
	AQ-22(♂) × YJ-d9A(♀) (F_{1c})	96	96.9	0.97
	AQ-22(♀) × YJ-d9A(♂) (F_{1d})	96	98	0.98
	F_1 pooled	192	97.5	0.98

*Numbers of larvae used in bioassays.

We also note that while the CYP9A186 of the wild-type *S. exigua* strain tested here had no detectable activity for abamectin, a naturally occurring mutation in its substrate recognition site has substantial activity and confers around 200-fold resistance (36, 42). We conclude that the amplification of CYP9A P450s in the spodopterans provides multiple opportunities for functional innovation and adaptive evolution to deal with otherwise toxic xenobiotics.

In contrast to the situation with the other compounds above, dozens of P450s from the CYP6, CYP9, CYP305, CYP321, CYP337, and CYP339 families across multiple insect species have previously been found to metabolize pyrethroids, with structural changes or increased expression often found to contribute to resistance (21, 34, 40, 41, 43, 54). Examples involving CYP9As in Lepidoptera include cases of resistance in *H. armigera* to esfenvalerate (34) and other pyrethroids (55, 56) and associations of three CYP9A members with moderate pyrethroid resistance in the light brown apple moth *Cydia pomonella* (57) and of other CYP9A copy number differences with deltamethrin resistance in *S. frugiperda* (37). Consistent with these studies, we found a majority of *S. exigua* and *S. frugiperda* CYP9As (8/10 and 11/14, respectively) showed detectable activity against esfenvalerate. Also consistent with the *H. armigera* data was our finding of a general bias toward metabolism to 4′- rather than 2′- hydroxy-esfenvalerate (34, 40, 41). However, there were also a few cases in the spodopterans of bias toward the 2′- product as well, and interestingly, all the CYP9As we found producing significant amounts of this product were closely related within a specific clade.

Given the similarity of many synthetic pyrethroids (SPs) to the naturally occurring plant defense compound pyrethrin (58), these CYP9A findings are consistent with the preadaptation hypothesis and further suggest that the relationship is enabled by the large number of options in the form of P450 genes with some level of activity (the so-called promiscuous activity) (59) against insecticidal SPs (45) which can then be improved upon by the selection imposed by heavy insecticide pressure (60). And the options appear to extend beyond the CYP9As, as multiple P450s with promiscuous activities for SPs have also been reported for the CYP6AE and CYP6B subfamilies in *H. armigera* (34, 40) and the CYP9J subfamily in the mosquito *Aedes aegypti* (61).

Table 2. Genetic association between the CYP9A gene cluster and esfenvalerate resistance in resistant strains of *S. exigua* and *S. frugiperda*

		CYP9A genotype		
Species	Strain/BC cohort	rr	rs	ss
S. exigua	WH-S			28
	FX-19	28		
	BC-untreated larvae (n = 18)		8	10
	BC-treated survivors (n = 20)		20	
S. frugiperda	YJ-d9A			28
	AQ-22	28		
	BC-untreated larvae (n = 20)		11	9
	BC-treated survivors (n = 20)		20	

BC = backcross. r and s represent the CYP9A haplotypes from the resistant and susceptible parental strains, respectively.

While the absolute numbers may be smaller, more than one CYP has also been found to metabolize several plant defense compounds. This was the case in our data for the furanocoumarins and was also found to apply to xanthotoxin and another plant defense compound, 2-tridecanone, as well as indoxacarb, imidacloprid and certain organochlorine insecticides, in the CYP6AE subfamily in *H. armigera* (24, 40). Our data thus generally support the proposition that having a multiplicity of metabolic options against plant defense compounds not only preadapts a species for the evolution of resistance against chemically related insecticides but, at least in some cases, may also facilitate its expansion onto new host plants (10, 24, 62, 63).

Although our activity data revealed a few striking cases of functional conservation, it also exposed many cases of functional divergence, both between orthologs in the two species and between duplicates in each. For example, SeCYP9A11 and SfCYP9A24 had the highest activities for imperatorin and xanthotoxin, respectively, but neither their species-specific duplicates nor their closest relatives in the other species had any detectable activity for the respective compounds. Widespread and rapid divergence in activity profiles might be expected given the sequence divergence we found between both orthologs and paralogs and the scope for even single amino acid changes in key active site residues to effect qualitative changes in substrate specificities (36, 42–44).

In addition to the divergence in activity profiles, there was also widespread variation in the organ-specific constitutive expression of the CYP9A genes. However, most of the expression variation lay between distantly related paralogs, where large differences in each organ and species were found, and there was more evidence of conservation between orthologs or species-specific duplicates than there had been in the activity data. For example, the SeCYP9A40 and SfCYP9A32 pair were both highly expressed in all four organs, and the two closely related pairs SeCYP9A11 and SfCYP9A26 and SeCYP9A27 and SfCYP9A27 were all preferentially expressed in the MG. The most striking example of divergence involved the orthologs SfCYP9A77 and SeCYP9A187 which were little and highly expressed in all four organs, respectively. Notably, the little expressed SfCYP9A77 had detectable

activity for esfenvalerate and moderate activity for indoxacarb, whereas the highly expressed SeCYP9A187 had no activity for any of the substrates tested, suggesting that we did not test its preferred in vivo substrate(s)—quite likely given the collectively broad range of known substrates for P450s (7, 64).

On the other hand, however, the other CYP9As that were highly expressed in all four detoxification organs did have high activity for at least one of the substrates we tested. In particular, SeCYP9A40 had the highest activity of all the *S. exigua* CYP9As for esfenvalerate and abamectin plus detectable activity against imperatorin, while its ortholog SfCYP9A32 had the highest activity of all *S. frugiperda* CYP9As for esfenvalerate plus relatively high activity for abamectin and indoxacarb. Since the compounds which they degrade represent very different chemotypes, this pair of orthologs would rate as generalist detoxifying P450s on the schema proposed by Li et al. (62) and Li et al. (65). In this respect, they are also reminiscent of two highly promiscuous human P450s which can metabolize a clear majority of the many drugs which they have been tested against (66, 67).

CYP9As such as SeCYP9A40 and SfCYP9A32 which are both highly expressed in all four detoxification organs and have relatively high esfenvalerate activity would be prime candidates for contributing to the "baseline" pyrethroid tolerance of the susceptible strains studied here. However, it does not follow that they would also be causally involved in the high-level resistance that had evolved in the field strains studied. They may have been, for example via nonsynonymous mutations further enhancing their pyrethroid detoxifying activity. Alternatively, the resistance could have been achieved by *cis*-acting regulatory changes in other members of the cluster, such as SeCYP9A11, SeCYP9A27, SfCYP9A28, and SfCYP9A29, which also have relatively high pyrethroid activity but were not previously expressed at high levels in all the relevant organs. Other explanations not directly involving the cluster might involve close linkage of the cluster to other potential resistance genes. However, this seems unlikely, for two reasons. First, the sodium channel gene that might mutate to confer target site resistance lies on a different chromosome (36, 39). Second, only two other members of the four superfamilies studied here lie within a megabase of the cluster in either species (*SI Appendix*, Fig. S4), and they are members of the CYP9AJ and CYP9G subfamilies which have not yet been implicated in pyrethroid resistance (17). Future work to identify the specific genes involved could utilize CRISPR/Cas9 knockouts or knockins of individual elements of the cluster in resistant or susceptible strains, respectively.

Two aspects of our data show that selection for esfenvalerate resistance could potentially produce cross-resistance to other insecticide classes. One is simply that, as noted, certain more generalist CYP9As in the cluster had pleiotropic activities against different insecticide classes. The other is that their close linkage, both to each other and to esfenvalerate resistance, suggests that strong selection for esfenvalerate resistance in the field would result in the hitchhiking of much of the cluster along with allele frequency changes in the specific members of the cluster targeted by the selection imposed by the esfenvalerate.

In conclusion, we have found considerable divergence in both the contents of the *CYP9A* cluster and in the sequences of individual *CYP9A* orthologs and recently arisen *CYP9A* duplicates in the spodopterans studied. We have also provided mechanistic evidence linking this genetic divergence to functional differences related to the detoxification of various host plant defense chemicals and insecticides. Our findings also highlight the potential which the *CYP9A* subfamily provides for the contemporaneous evolution of cross-resistance to multiple insecticide chemotypes. As such, they both shed light on coevolutionary processes brought into play by the interactions between insect herbivores and their hosts and bring unique perspectives to bear on pest and pesticide management practices for a major group of insect pests.

Materials and Methods

Insects and Chemicals. The two wild-type strains used were the WH-S *S. exigua* strain, which was originally collected from Wuhan (Hubei, China) in 1998 and provided to us by the Wuhan Institute of Vegetables (68), and the YJ-19 *S. frugiperda* strain, which we collected from maize in Yuanjiang (Yunan, China) in 2019 (69). Both strains had been maintained in the laboratory without exposure to insecticides since their collection from the field. Both are considered to be esfenvalerate-susceptible strains (68, 69), although YJ-19 shows higher tolerance to esfenvalerate than WH-S (*SI Appendix*, Table S4). This is likely because it was collected from the field more recently and subsequently had fewer generations in the laboratory without exposure to insecticides in which any initial resistance could have decayed (70). The WH-d9A and YJ-d9A strains were derived from WH-S and YJ-19 by knocking out the CYP9A gene cluster with the CRISPR-Cas9 genome editing tool. The two pyrethroid-resistant strains used were the FX-19 *S. exigua* strain, which was collected from chrysanthemum fields in the Fenxian district of Shanghai in January 2019 (42) and the AQ-22 *S. frugiperda* strain, which was collected from maize fields in Anqing (Anhui, China) in August 2022 (*SI Appendix*, Table S4). Adults reared from each of these latter collections were mated at random in their respective cages and larvae from F_1 and F_2 progeny were used in bioassays and genetic analysis.

Chemicals used in bioassays included xanthotoxin (98%, J&K Chemical), imperatorin (95%, Shanghai Yuanye Biological Technology, Shanghai), esfenvalerate (99%, Aladdin Industrial Corporation), technical grade emamectin benzoate and chlorfenapyr (74.1% and 98.2% TC, respectively, Bayer China, Beijing, China), and indoxacarb (97.6% TC, Jingbo Agrochemicals Technology, Binzhou, China). Formulated versions of other insecticides used in bioassays included spinosad (25 g/L SC, Dow Agrosciences, Indiana, USA), chlorantraniliprole (200 g/L SC, DuPont Agricultural Chemicals, Delaware, USA), abamectin (18 g/L EC, Henan Yongguanqiaodi Agricultural Technology, Henan, China), and chlorpyrifos (400 g/L EC, Sinon Chemical, Shanghai).

Chemicals used in in vitro biochemistry were xanthotoxin, imperatorin (99.98%, CAS 298-81-7, and 98%, CAS 482-44-0, respectively, MedChemExpress), emamectin benzoate (EB, ~93.4% B1a, CAS: 155569-91-8, 98%, Sigma-Aldrich, St. Louis, Missouri, USA), abamectin (B1a, CAS: 65195-55-3, 97%, Toronto Research Chemicals, North York, Canada), s-indoxacarb (CAS: 173584-44-6, 99.3%, ChemService, West Chester, Pennsylvania, USA), esfenvalerate (CAS: 66230-04-4, 99%, Dr. Ehrensorfer, Augsburg, Germany), and the UPLC solvents ammonium acetate, formic acid, and acetonitrile (Thermo Fisher Scientific, Pittsburgh, Pennsylvania).

CRISPR-Cas9 Knockouts. Knockouts of the CYP9A gene cluster in each species were produced in the WH-S and YJ-19 strains using methods based on previously described work (24, 36). Zuo et al. (36) had also created a knockout of the CYP9A cluster in *S. exigua* but the current study used an esfenvalerate-susceptible rather than resistant strain and primers that had been optimized since that work. Briefly, two sgRNAs targeting the HD and tail genes of the clusters (*SfCYP9A60* and *SfCYP9A32* of *S. frugiperda* and *SeCYP9A98* and *SeCYP9A40* of *S. exigua*) were designed according to their respective genome sequences [GenBank Nos GCF_011064685.1 (39) and GCA_011316535.1 (36)]. The sgRNAs were synthesized by PCR using the GeneArt™ Precision gRNA Synthesis Kit following the manufacturer's instructions (Thermo Fisher Scientific) and the primers detailed in *SI Appendix*, Table S5. Mixtures were then prepared containing the respective sgRNAs (final concentrations each 300 ng/μL) for each species and the Cas9 protein (final concentration 200 ng/μL, TrueCut Cas9 Protein *v2*, Thermo Fisher Scientific). Within 2 h of its preparation approximately 1 nL of the corresponding mixture was injected into freshly laid eggs of each species using a FemtoJet and InjectMan NI 2 microinjection system (Eppendorf, Hamburg, Germany). Injected eggs were placed in an incubator at 26 ± 1 °C, 50 to 70% relative humidity for hatching.

To detect the knockouts in the crossing programs below, PCR fragments flanking the sgRNA target sites were amplified from genomic DNA (gDNA) of individuals using gene-specific primer pairs (*SI Appendix*, Table S5). In *S. frugiperda*, forward and reverse primers located in *SfCYP9A60* (60F) and *SfCYP9A32* (32R), respectively, generated an ~800 bp fragment of gDNA if the cluster was deleted. Two pairs of primers specific for the *SfCYP9A59* and *SfCYP9A28* genes internal to the cluster

(59F/59R and 28F/28R, respectively; *SI Appendix*, Table S5) were then used to distinguish homozygous and heterozygous knockouts. 59F/59R and 28F/28R generated PCR products of ~900 bp and ~700 bp, respectively. Genotypes were initially discriminated according to the banding patterns of their PCR-amplified products and then confirmed by Sanger sequencing. *S. exigua* knockouts were detected in a similar manner, except that the flanking primers (98F/40R; *SI Appendix*, Table S5) targeted its *SeCYP9A98* and *SeCYP9A40* genes and generated a ~1,200-bp PCR product if the cluster was deleted, and three pairs of homo- vs. heterozygous genotyping primers (186F/186R, 107F/107R, 9F/9R; *SI Appendix*, Table S5) were used against the internal *SeCYP9A186*, *SeCYP9A107*, and *SeCYP9A9* genes, respectively, generating ~1,100 bp, ~ 500 bp, and ~ 300 bp products, respectively.

The crossing program to produce a homozygous knockout *S. exigua* strain was again based on that used by Zuo et al. (36). Briefly, 10 G_1 larvae from each of 30 single pair matings of G_0 moths were genotyped as above and families with the knockout mutations were retained. Heterozygous G_1 adults from one of those families were then mass crossed. Then, the homozygous knockout G_2 moths were mass crossed to establish the homozygous strain. The G_1 and G_2 moths were genotyped nondestructively before mating by removing one hind leg for PCR and sequence analysis. A similar crossing scheme was used to create a homozygous knockout strain of *S. frugiperda*.

Bioassays. Diet incorporation bioassays comparing the susceptibilities of the knockout and parental strains against the phytochemicals xanthotoxin and imperatorin were conducted under the same conditions for the two species. Various concentrations of each chemical were mixed thoroughly with liquid artificial diet (68) at approx. 60 °C using an electric mixer. The mixture (1 mL) was then dispensed into each well of a 24-well plate (GongDong Medical Technology, Taizhou, China) before being cooled and solidified. A single unfed neonate was put in each well, and 24 to 48 larvae of each strain were tested for each of five to seven concentrations of each chemical. Mortality was recorded after 120 h. Larvae were scored as dead if they died or did not reach the third instar by the end of bioassays.

Diet surface overlay bioassays as described in Shi et al. (69) and Zuo et al. (36) were used to test the susceptibilities of the knockout and parental strains of the two species against the eight insecticides. Stocks of 10 g/L emulsifiable concentrates were prepared for each of esfenvalerate, emamectin benzoate, chlorfenapyr and indoxacarb by blending the purchased samples with acetone and Triton X-100 (final concentration in the emulsifiable concentrate: 10%, *w*/*w*). The stocks of abamectin, spinosad, chlorantraniliprole, and chlorpyrifos were simply the formulated versions purchased. Serial dilutions of all stocks were prepared with distilled water containing 0.1% (*w*/*v*) Triton X-100. Then, 100 μL of insecticide solution was applied evenly to the surface of 1.2 mL of freshly prepared and solidified diet in each well of a 24-well plate. One early-third instar larva was placed in each well after the applied solution had dried at room temperature. Forty-eight larvae of each strain were tested at each of five to eight concentrations of each insecticide. Mortality was recorded after 72 h for both *S. exigua* and *S. frugiperda*. Larvae were scored as dead if they did not respond after gentle prodding with a brush.

Probit analysis of the mortality data from all the bioassays used the PoloPlus program (LeOra Software LLC, Cape Girardeau, MO, USA). Two LC_{50} values were considered significantly different if their 95% fiducial limits did not overlap (71).

Quantitative reverse-transcription polymerase chain reaction (qRT-PCR). The qRT-PCR assays used to assess the spatial expression patterns and relative expression levels of the various *S. exigua* and *S. frugiperda* CYP9A genes were performed as previously described (36, 40).

Total RNA was isolated from the MG, FB, MT, and HD of fifth instars of WH-S and sixth instars of YJ-19 (24 h to 48 h old) by TRIzol. Tissues from five individuals were pooled as one sample. A total of 1,000 ng of RNA was used for the first strand complementary DNA (cDNA) synthesis by using HiScript III RT SuperMix for the qPCR Reverse Transcriptase kit (Vazyme, Nanjing, China) following the manufacturer's instructions. Data were normalized to the geometric mean of two housekeeping genes (*β-actin* and *GADPH* of *S. exigua*; *EF1α* and *GADPH* of *S. frugiperda*). Each quantitative RT-PCR experiment consisted of 6 to 8 independent biological replicates, with two technical replicates for each biological replicate. Melt curves (65) and sequencing were used to check for nonspecific amplification. The efficiency of PCR for each primer pair was assessed using serially diluted cDNA.

The copy number of the *SeCYP9A9* gene was assessed by quantitative PCR using essentially the same methods as above but with gDNA as the template as per Puinean et al. (66). The two single copy genes used for normalizing *SeCYP9A9* expression values were the voltage-gated sodium channel gene and *SeCYP9A107*. The primer sequences are given in *SI Appendix*, Table S5.

Heterologous Expression. The open reading frames of all 14 *S. frugiperda* and 10 *S. exigua* CYP9A genes were cloned from the wild-type YJ-19 and WH-S strains, respectively. The primers used for cloning (*SI Appendix*, Table S5) were designed according to the GenBank reference genomes of *S. exigua* [GCA_011316535.1 (36)] and *S. frugiperda* [GCA_011064685.2 (39) and GCA_019297735.1 (37)]. The official names of all 24 CYP9A genes were confirmed by the International P450 Nomenclature Committee.

All 24 CYP9A genes were inserted into the pFastBac1 vector and heterologously expressed in Sf9 cells with the Bac-to-Bac baculovirus expression system (Invitrogen, Carlsbad, California, USA) as previously described (40). The pFastBac1 vector with no insert DNA was used to produce a control virus. The cytochrome P450 reductases of *S. frugiperda* and *S. exigua* (Sf-CPR and Se-CPR, GenBank accession nos XM_035580124.2 and (MN179471, respectively), were coexpressed with the P450s of the same species under multiplicities of infection (MOIs) of 1 and 2 for the CPR and P450, respectively. Protein from cells coinfected with the control virus and CPR under the same MOIs was used as a noninsertion control. Microsomes of infected cells were purified by differential centrifugation (41) and quantified by the Bradford method (72). The recombinant P450 was identified and quantified by reduced CO-difference spectral assay (73).

Enzyme Assays. The catalytic activities of each heterologously expressed P450 against some of the pesticides and the two plant allelochemicals were confirmed in qualitative tests and then compared in quantitative assays.

The reaction mixture for the qualitative assays contained 0.2 mg microsomes, an nicotinamide adenine dinucleotide phosphate (NADPH) regeneration system (final concentrations of 1.3 mM $NADP^+$, 3.3 mM glucose-6-phosphate and 3.3 mM $MgCl_2$, plus 0.4 U/mL glucose-6-phosphate dehydrogenase) and substrate (final concentration of 50 μM esfenvalerate, 20 μM xanthotoxin or 10 μM abamectin, indoxacarb or imperatorin) in 200 μL 0.1 M potassium phosphate buffer, pH 7.4. All substrates were prepared from stock solutions freshly dissolved in dimethyl sulfoxide (DMSO) at final DMSO concentrations ≤ 1%. Three replicate reactions were tested with each of two batches of microsomes for each enzyme. Reactions were prewarmed at 30 °C for 5 min and started by adding substrate. After a 1-h incubation in an orbital shaking incubator at 30 °C and 1,200 rpm, the reactions were stopped by adding 200 μL acetonitrile. Then, 600 μL dilution buffer [50% acetonitrile and 50% potassium phosphate buffer (pH 7.4)] was added to each sample, which was then incubated for a further 10 min at 30 °C and 1,200 rpm. Samples were analyzed by ultraperformance liquid chromatography–mass spectrometry/mass spectrometry (UPLC-MS/MS) immediately after clarification by centrifugation (15,000 × g, 10 min) and filtration (0.22 μm). The clearance of substrate or, in the case of esfenvalerate, the formation of the metabolites 2′- and 4′-hydroxy-esfenvalerate was monitored, with external standards used in every case. Activity for the substrate in question was defined as conversion above the lower limit of detection (LOD) and significantly higher than that of the noninsertion control run at the same time.

Quantitative comparisons between active P450s were made using the same protocols, except that 20 pmol P450 (as defined by reduced CO-difference analysis) was used, or, for abamectin and emamectin benzoate, 10 pmol and a reaction time of 45 min. Activity was calculated after subtracting any background (i.e., any activity of noninsertion controls with equivalent total protein) and expressed as pmol substrate consumed or metabolite produced/min/pmol P450. The recovery rates of the substrates using recombinant microsomal protein without the NADPH regeneration system were close to 100%.

UPLC-MS/MS. The 2′- and 4′-hydroxy-esfenvalerate, xanthotoxin, indoxacarb, and abamectin were monitored as previously described (24, 36, 40). For imperatorin, 1 μL samples were separated on a BEH C8 column (2.1 × 50 mm, 1.7 μm particle size; Waters, Milford, Massachusetts, USA) using an Acquity UPLC system (I-Class; Waters) and eluted with acetonitrile (A) and 1 mM ammonium acetate (B). The gradient elution program was 0 min A:B 10:90; 0.3 min A:B 10:90; 2 min A:B 95:5; 3 min A:B 95:5; 3.1 min A:B 10:90; and 5 min A:B 10:90, and the flow rate was 0.3 mL/min. The imperatorin was detected on a tandem triple quadrupole mass spectrometer (Xevo TQ-S micro; Waters) run in positive ESI and multiple reaction monitoring (MRM) modes, with the MRM transitions 271 > 203.2 and 271 > 147.1 used for quantification of imperatorin and confirmation

of its identity. The LOD for imperatorin conversion under these conditions was 0.06 pmol/min/pmol P450.

Genetic Analyses. To determine the mode of inheritance of esfenvalerate resistance in field strains of the two species, individuals from FX-19 and AQ-22 were treated with esfenvalerate at a high dose (100 ppm), and then, 15 survivors of each sex were reciprocally mass crossed to 15 individuals of a conspecific susceptible strain. The highly susceptible wild-type WH-S strain was used in the case of *S. exigua,* but the YJ-d9A knockout strain was preferred over the wild-type YJ-19 strain for *S. frugiperda* because, as noted, the latter showed some tolerance to esfenvalerate (*SI Appendix*, Table S4). The survival rate of susceptible strains, resistant field strains, and hybrid F_1 progenies from two reciprocal crosses was then determined at the diagnostic esfenvalerate concentration (20 ppm for *S. exigua* and 35 ppm for *S. frugiperda*). The dominance parameter *h* was calculated as (survival rate of F_1 − survival rate of susceptible strain)/(survival rate of resistant strain − survival rate of susceptible strain).

To test for linkage between the *CYP9A* cluster and esfenvalerate resistance in each species, 15 of the male F_1 survivors above were mass-backcrossed with 15 females of the corresponding susceptible strain. The backcross progeny (BC) were treated with the diagnostic concentration of esfenvalerate and gDNA from the survivors and untreated BC individuals were extracted for genotyping. In the case of *S. exigua*, a pair of primers (qCYP9A186-F/R, *SI Appendix*, Table S5) was used to amplify a 282 bp fragment of *SeCYP9A186* containing an informative single nucleotide polymorphism (T346G), which was then sequenced. In the case of *S. frugiperda*, two pairs of primers (60F/32R and 59F/59R, *SI Appendix*, Table S5) were used to diagnose the presence/absence of the *CYP9A* cluster from the banding patterns of their PCR products.

Data, Materials, and Software Availability. All study data are included in the article and/or supporting information.

ACKNOWLEDGMENTS. This work was funded by the National Key R&D Program of China (grant no. 2022YFD1400901).

Author affiliations: [a]College of Plant Protection, Nanjing Agricultural University, Nanjing, Jiangsu 210095, China; and [b]Applied Biosciences, Macquarie University, Sydney, NSW 2109, Australia

1. L. Després, J. David, C. Gallet, The evolutionary ecology of insect resistance to plant chemicals. *Trends Ecol. Evol.* **22**, 298–307 (2007).
2. P. P. Edger *et al.*, The butterfly plant arms-race escalated by gene and genome duplications. *Proc. Natl. Acad. Sci. U.S.A.* **112**, 8362–8366 (2015).
3. H. M. Heidel-Fischer, H. Vogel, Molecular mechanisms of insect adaptation to plant secondary compounds. *Curr. Opin. Insect Sci.* **8**, 8–14 (2015).
4. R. V. Rane *et al.*, Detoxifying enzyme complements and host use phenotypes in 160 insect species. *Curr. Opin. Insect Sci.* **31**, 131–138 (2019).
5. S. Ahn, H. Vogel, D. G. Heckel, Comparative analysis of the UDP-glycosyltransferase multigene family in insects. *Insect Biochem. Mol. Biol.* **42**, 133–147 (2012).
6. A. A. Enayati, H. Ranson, J. Hemingway, Insect glutathione transferases and insecticide resistance. *Insect Mol. Biol.* **14**, 3–8 (2005).
7. R. Feyereisen, "Insect CYP genes and P450 enzymes" in *Insect Molecular Biology and Biochemistry*, L. I. Gilbert, Ed. (Academic Press, 2012), pp. 236–316.
8. J. G. Oakeshott, C. Claudianos, P. M. Campbell, R. D. Newcomb, R. J. Russell, "Biochemical genetics and genomics of insect esterases" in *Comprehensive Molecular Insect Science*, L. I. Gilbert, Ed. (Elsevier, 2005), pp. 309–381.
9. H. O. Aidlin *et al.*, Molecular evolution of the glutathione s-transferase family in the *Bemisia tabaci* species complex. *Genome Biol. Evol.* **12**, 3857–3872 (2020).
10. C. Bass *et al.*, Gene amplification and microsatellite polymorphism underlie a recent insect host shift. *Proc. Natl. Acad. Sci. U.S.A.* **110**, 19460–19465 (2013).
11. B. Calla *et al.*, Cytochrome P450 diversification and hostplant utilization patterns in specialist and generalist moths: Birth, death and adaptation. *Mol. Ecol.* **26**, 6021–6035 (2017).
12. A. Gouin *et al.*, Two genomes of highly polyphagous lepidopteran pests (*Spodoptera frugiperda*, Noctuidae) with different host-plant ranges. *Sci. Rep.* **7**, 11816 (2017).
13. K. S. Singh *et al.*, The genetic architecture of a host shift: An adaptive walk protected an aphid and its endosymbiont from plant chemical defenses. *Sci. Adv.* **6**, a1070 (2020).
14. L. M. Field, R. L. Blackman, C. Tyler-Smith, A. L. Devonshire, Relationship between amount of esterase and gene copy number in insecticide-resistant *Myzus persicae* (Sulzer). *Biochem J.* **339**, 737–742 (1999).
15. J. Haas *et al.*, Phylogenomic and functional characterization of an evolutionary conserved cytochrome P450-based insecticide detoxification mechanism in bees. *Proc. Natl. Acad. Sci. U.S.A.* **119**, e2089117177 (2022).
16. N. B. Hardy, D. A. Peterson, L. Ross, J. A. Rosenheim, Does a plant–eating insect's diet govern the evolution of insecticide resistance? Comparative tests of the pre-adaptation hypothesis *Evol. Appl.* **11**, 739–747 (2018).
17. R. Nauen, C. Bass, R. Feyereisen, J. Vontas, The role of cytochrome P450s in insect toxicology and resistance. *Annu. Rev. Entomol.* **67**, 105–124 (2022).
18. C. T. Zimmer *et al.*, Neofunctionalization of duplicated P450 genes drives the evolution of insecticide resistance in the brown planthopper. *Curr. Biol.* **28**, 268–274 (2018).
19. C. Manjon *et al.*, Unravelling the molecular determinants of bee sensitivity to neonicotinoid insecticides. *Curr. Biol.* **28**, 1137–1143 (2018).
20. F. Hilliou, T. Chertemps, M. Maïbèche, G. Le Goff, Resistance in the genus *Spodoptera*: Key insect detoxification genes. *Insects* **12**, 544 (2021).
21. R. Nauen, C. T. Zimmer, J. Vontas, Heterologous expression of insect P450 enzymes that metabolize xenobiotics. *Curr. Opin. Insect Sci.* **43**, 78–84 (2021).
22. M. Vandenhole, W. Dermauw, T. Van Leeuwen, Short term transcriptional responses of P450s to phytochemicals in insects and mites. *Curr. Opin. Insect Sci.* **43**, 117–127 (2021).
23. M. Sasabe, Z. Wen, M. R. Berenbaum, M. A. Schuler, Molecular analysis of CYP321A1, a novel cytochrome P450 involved in metabolism of plant allelochemicals (furanocoumarins) and insecticides (cypermethrin) in *Helicoverpa zea*. *Gene* **338**, 163–175 (2004).
24. H. Wang *et al.*, CYP6AE gene cluster knockout in *Helicoverpa armigera* reveals role in detoxification of phytochemicals and insecticides. *Nat. Commun.* **9**, 4820 (2018).
25. W. Dermauw *et al.*, A link between host plant adaptation and pesticide resistance in the polyphagous spider mite *Tetranychus urticae*. *Proc. Natl. Acad. Sci. U.S.A.* **110**, 393–394 (2013).
26. A. Alyokhin, Y. H. Chen, Adaptation to toxic hosts as a factor in the evolution of insecticide resistance. *Curr. Opin. Insect Sci.* **21**, 33–38 (2017).
27. H. T. Gordon, Nutritional factors in insect resistance to chemicals. *Annu. Rev. Entomol.* **6**, 27–54 (1961).
28. G. J. Kergoat *et al.*, A novel reference dated phylogeny for the genus *Spodoptera* Guenée (Lepidoptera: Noctuidae: Noctuinae): New insights into the evolution of a pest-rich genus. *Mol. Phylogenet. Evol.* **161**, 107161 (2021).
29. D. Boaventura, M. Martin, A. Pozzebon, D. Mota-Sanchez, R. Nauen, Monitoring of target-site mutations conferring insecticide resistance in *Spodoptera frugiperda*. *Insects* **11**, 545 (2020).
30. F. Guan *et al.*, Whole-genome sequencing to detect mutations associated with resistance to insecticides and Bt proteins in *Spodoptera frugiperda*. *Insect Sci.* **28**, 627–638 (2021).
31. H. Teng, Y. Zuo, Z. Jin, Y. Wu, Y. Yang, Associations between acetylcholinesterase-1 mutations and chlorpyrifos resistance in beet armyworm, *Spodoptera exigua*. *Pest. Biochem. Physiol.* **184**, 105105 (2022).
32. M. Giraudo *et al.*, Cytochrome P450s from the fall armyworm (*Spodoptera frugiperda*): Responses to plant allelochemicals and pesticides. *Insect Mol. Biol.* **24**, 115–128 (2015).
33. D. Amezian, R. Nauen, G. Le Goff, Comparative analysis of the detoxification gene inventory of four major *Spodoptera* pest species in response to xenobiotics. *Insect Biochem. Mol. Biol.* **138**, 103646 (2021).
34. Y. Shi, Q. Jiang, Y. Yang, R. Feyereisen, Y. Wu, Pyrethroid metabolism by eleven *Helicoverpa armigera* P450s from the CYP6B and CYP9A subfamilies. *Insect Biochem. Mol. Biol.* **135**, 103597 (2021).
35. D. Boaventura, B. Buer, N. Hamaekers, F. Maiwald, R. Nauen, Toxicological and molecular profiling of insecticide resistance in a Brazilian strain of fall armyworm resistant to Bt Cry1 proteins. *Pest Manag. Sci.* **77**, 3713–3726 (2021).
36. Y. Zuo *et al.*, Genome mapping coupled with CRISPR gene editing reveals a P450 gene confers avermectin resistance in the beet armyworm. *PLoS Genet.* **17**, e1009680 (2021).
37. S. Gimenez *et al.*, Adaptation by copy number variation increases insecticide resistance in the fall armyworm. *Commun. Biol.* **3**, 664 (2020).
38. T. Cheng *et al.*, Genomic adaptation to polyphagy and insecticides in a major East Asian noctuid pest. *Nat. Ecol. Evol.* **1**, 1747–1756 (2017).
39. H. Xiao *et al.*, The genetic adaptations of fall armyworm *Spodoptera frugiperda* facilitated its rapid global dispersal and invasion. *Mol. Ecol. Resour.* **20**, 1050–1068 (2020).
40. Y. Shi *et al.*, Phylogenetic and functional characterization of ten P450 genes from the *CYP6AE* subfamily of *Helicoverpa armigera* involved in xenobiotic metabolism. *Insect Biochem. Mol. Biol.* **93**, 79–91 (2018).
41. Y. Shi *et al.*, Involvement of CYP2 and mitochondrial clan P450s of *Helicoverpa armigera* in xenobiotic metabolism. *Insect Biochem. Mol. Biol.* **140**, 103696 (2022).
42. H. Teng *et al.*, High frequency of ryanodine receptor and cytochrome P450 CYP9A186 mutations in insecticide-resistant field populations of *Spodoptera exigua* from China. *Pest. Biochem. Physiol.* **186**, 105153 (2022).
43. Y. Shi *et al.*, Single amino acid variations drive functional divergence of cytochrome P450s in *Helicoverpa* species. *Insect Biochem. Mol. Biol.* **146**, 103796 (2022).
44. Y. Shi *et al.*, Roles of the variable P450 substrate recognition sites SRS1 and SRS6 in esfenvalerate metabolism by CYP6AE subfamily enzymes in *Helicoverpa armigera*. *Insect Biochem. Mol. Biol.* **127**, 103486 (2020).
45. E. d'Alencon *et al.*, Extensive synteny conservation of holocentric chromosomes in Lepidoptera despite high rates of local genome rearrangements. *Proc. Natl. Acad. Sci. U.S.A.* **107**, 7680–7685 (2010).
46. R. Feyereisen, Arthropod CYPomes illustrate the tempo and mode in P450 evolution. *Biochim. Biophys. Acta Proteins Proteom.* **1814**, 19–28 (2011).
47. R. T. Good *et al.*, The molecular evolution of cytochrome P450 genes within and between *Drosophila* species. *Genome Biol. Evol.* **6**, 1118–1134 (2014).
48. W. Dermauw, T. Van Leeuwen, R. Feyereisen, Diversity and evolution of the P450 family in arthropods. *Insect Biochem. Mol. Biol.* **127**, 103490 (2020).
49. K. Darragh, D. R. Nelson, S. R. Ramírez, The birth–and-death evolution of cytochrome P450 genes in bees. *Genome Biol. Evol.* **13**, evab261 (2021).
50. G. E. Batiha *et al.*, *Rhus coriaria* L. (Sumac), a versatile and resourceful food spice with cornucopia of polyphenols. *Molecules* **27**, 5179 (2022).
51. T. K. Walsh *et al.*, Determinants of insecticide resistance evolution: Comparative analysis among heliothines. *Annu. Rev. Entomol.* **67**, 387–406 (2022).
52. CABI, *Spodoptera exempta (black armyworm). Invasive Species Compendium* (CAB International, Wallingford, UK, 2020).
53. M. Riga *et al.*, Abamectin is metabolized by CYP392A16, a cytochrome P450 associated with high levels of acaricide resistance in *Tetranychus urticae*. *Insect Biochem. Mol. Biol.* **46**, 43–53 (2014).

54. E. Katsavou *et al.*, Functionally characterized arthropod pest and pollinator cytochrome P450s associated with xenobiotic metabolism. *Pest. Biochem. Physiol.* **181**, 105005 (2022).
55. Y. Yang, L. Yue, S. Chen, Y. Wu, Functional expression of *Helicoverpa armigera CYP9A12* and *CYP9A14* in *Saccharomyces cerevisiae*. *Pest. Biochem. Physiol.* **92**, 101–105 (2008).
56. Y. Yang, S. Chen, S. Wu, L. Yue, Y. Wu, Constitutive overexpression of multiple cytochrome P450 genes associated with pyrethroid resistance in *Helicoverpa armigera*. *J. Econ. Entomol.* **99**, 1784–1789 (2006).
57. P. Li *et al.*, Metabolic functional redundancy of the CYP9A subfamily members leads to P450-mediated lambda-cyhalothrin resistance in *Cydia pomonella*. *Pest Manag. Sci.* **79**, 1452–1466 (2022).
58. M. S. Crossley, W. E. Snyder, N. B. Hardy, Insect–plant relationships predict the speed of insecticide adaptation. *Evol. Appl.* **14**, 290–296 (2021).
59. P. J. O'Brien, D. Herschlag, Catalytic promiscuity and the evolution of new enzymatic activities. *Chem. Biol.* **6**, R91–R105 (1999).
60. S. S. Ibrahim *et al.*, Allelic variation of cytochrome P450s drives resistance to bednet insecticides in a major malaria vector. *PLoS Genet.* **11**, e1005618 (2015).
61. B. J. Stevenson, P. Pignatelli, D. Nikou, M. J. Paine, Pinpointing P450s associated with pyrethroid metabolism in the dengue vector, *Aedes aegypti*: Developing new tools to combat insecticide resistance. *PLoS Neglect. Trop. Dis.* **6**, e1595 (2012).
62. W. Li, M. A. Schuler, M. R. Berenbaum, Diversification of furanocoumarin-metabolizing cytochrome P450 monooxygenases in two papilionids: Specificity and substrate encounter rate. *Proc. Natl. Acad. Sci. U.S.A.* **100**, 14593–14598 (2003).
63. W. Mao, M. A. Schuler, M. R. Berenbaum, CYP9Q-mediated detoxification of acaricides in the honey bee (*Apis mellifera*). *Proc. Natl. Acad. Sci. U.S.A.* **108**, 12657–12662 (2011).
64. M. A. Schuler, M. R. Berenbaum, Structure and function of cytochrome P450s in insect adaptation to natural and synthetic toxins: Insights gained from molecular modeling. *J. Chem. Ecol.* **39**, 1232–1245 (2013).
65. X. Li, J. Baudry, M. R. Berenbaum, M. A. Schuler, Structural and functional divergence of insect CYP6B proteins: From specialist to generalist cytochrome P450. *Proc. Natl. Acad. Sci. U.S.A.* **101**, 2939–2944 (2004).
66. T. Lynch, A. Price, The effect of cytochrome P450 metabolism on drug response, interactions, and adverse effects. *Am. Fam. Physician.* **76**, 391–396 (2007).
67. M. Zhao *et al.*, Cytochrome P450 enzymes and drug metabolism in humans. *Int. J. Mol. Sci.* **22**, 12808 (2021).
68. W. Che, T. Shi, Y. Wu, Y. Yang, Insecticide resistance status of field populations of *Spodoptera exigua* (Lepidoptera: Noctuidae) from China. *J. Econ. Entomol.* **106**, 1855–1862 (2013).
69. T. Shi, P. Tang, X. Wang, Y. Yang, Y. Wu, CRISPR-mediated knockout of nicotinic acetylcholine receptor (nachr) α6 subunit confers high levels of resistance to spinosyns in *Spodoptera frugiperda*. *Pest. Biochem. Physiol.* **187**, 105191 (2022).
70. Y. Han *et al.*, Variation in P450-mediated fenvalerate resistance levels is not correlated with *CYP337B3* genotype in Chinese populations of *Helicoverpa armigera*. *Pestic. Biochem. Physiol.* **121**, 129–135 (2015).
71. M. E. Payton, M. H. Greenstone, N. Schenker, Overlapping confidence intervals or standard error intervals: What do they mean in terms of statistical significance? *J. Insect Sci.* **3**, 34 (2003).
72. M. M. Bradford, A rapid and sensitive method for the quantitation of microgram quantities of protein utilizing the principle of protein-dye binding. *Anal. Biochem.* **72**, 248–254 (1976).
73. T. Omura, R. Sato, The carbon monoxide-binding pigment of liver microsomes. I. Evidence for its hemoprotein nature. *J. Biol. Chem.* **239**, 2370–2378 (1964).